Biomimetic behavior of synthetic particles: from microscopic randomness to macroscopic control

Yiying Hong,*[a] Darrell Velegol,*[b] Neetu Chaturvedi[c] and Ayusman Sen*[d]

Received 28th August 2009, Accepted 17th November 2009
First published as an Advance Article on the web 22nd December 2009
DOI: 10.1039/b917741h

Randomness is an inherent property of biological systems. In contrast, randomness has been mostly avoided in designing synthetic or artificial systems. Particularly, in designing micro/nano-motors, some researchers have successfully used external fields to gain deterministic control over the directionality of the objects, which otherwise move in completely random directions due to Brownian motion. However, a partial control that preserves a certain degree of randomness can be very useful in certain applications of micro/nano-motors. In this Perspective we review the current progress in establishing autonomous motion of micro/nano-particles that possess *controlled randomness*, provide insight into the phenomena where macroscopic order originates from microscopic disorder and discuss the resemblance between these artificial systems and biological emergent/collective behaviors.

1. Introduction

What is it like to live in a world where non-biological, microscopic machines give biological responses? Imagine molecular or colloidal scale sensing robots tracking down a source of petroleum underground by chemotaxis, signaling each other when they find the oil by a collective quorum sensing mechanism, recording local environmental information, loading micro-droplets of the petroleum from its dark residence by a pseudo-receptor-mediated process, and transporting them to ground level by phototaxis. In 1959 when Nobel Laureate Richard Feynman presented the idea of atomic scale surgical robots in his talk "There's Plenty of Room at the Bottom", few thought the ideas were serious. Half a century has passed. The concept of building nano-scale machines has been revisited by a few groups of scientists, and we now have the first generation of self-propelled micro/nano-swimmers[1] that move by catalytically converting chemical energy to mechanical power. Of these tiny machines, some can respond to external signals[2–4] while some can carry and drop cargo.[4,5] Feynman's wildest dream is arriving. Of course, moving a molecular or nano-scale machine is not like driving an automobile; the randomizing effect of Brownian motion becomes significant at small length scales. But after working for years to deliberately eliminate random motions and bring deterministic directionality to our micro/nano-motors systems, we asked ourselves: is it really necessary—or even desirable—to eliminate randomness completely?

[a] *Department of Chemistry, Pennsylvania State University, University Park, PA 16802, USA. E-mail: yuh118@chem.psu.edu*
[b] *Department of Chemical Engineering, Pennsylvania State University, University Park, PA 16802, USA. E-mail: velegol@psu.edu*
[c] *Department of Chemical Engineering, Pennsylvania State University, University Park, PA 16802, USA*
[d] *Department of Chemistry, Pennsylvania State University, University Park, PA 16802, USA. E-mail: asen@chem.psu.edu*

Yiying Hong

Yiying Hong was born in Xiamen, China. She received her BS in organic chemistry from Peking University. She is currently working towards her PhD under the guidance of Prof. Ayusman Sen at the Pennsylvania State University. Her research interests include hydrogel-assisted heterogeneous catalysis and the design and improvements on self-propelled micro/nano-motors and micro-pumps.

Darrell Velegol

Darrell Velegol attended West Virginia University for his BS in Chemical Engineering. He earned his PhD in Chemical Engineering at Carnegie Mellon University in 1997, and he continued on with a post-doc in the Center for Light Microscope Imaging and Biotechnology at CMU. In June 1999 he joined Penn State University, where he is currently Professor of Chemical Engineering. His research group investigates the fabrication of colloidal assemblies and devices, using a wide range of experimental and modeling approaches for understanding interparticle forces, electrokinetics, and particle sorting processes.

Unpredictability, a quality originating from randomness, constitutes a major part of our life. We can never predict the next move of a fly even though we have very good understanding about its response to environmental stimuli.[6] Prey would be much less efficient at running away from a predator if they moved in a straight line. In the microbial world, bacteria undergo chemotaxis, phototaxis and aerotaxis[7–10] by gaining directionality upon the presence of stimuli gradients while maintaining their random motion. Andrew and Insall[11] in their recent publication about chemotaxis in shallow gradients point out that a biased random motion is sometimes more effective and desirable in a fluctuating environment, or to handle multiple and conflicting signals. So what would happen if we make use of randomness instead of eliminating it? Using our previous example of petroleum-sensing/locating nano-robot, once a robot finds oil, we do not want all the robots to gather at this spot. What we want is a mapping of the oil reservoirs of the entire region. For this to happen, the robots not only have to respond to the oil-detected signals from other robots, but also need to sample the terrain in order to find new oil pockets. Eventually, bigger reservoirs will attract more robots, which in turn amplify the signals. The same holds true for most sensor applications, that randomness is essential to ensure thorough sensing.

Currently there are mainly two types of movements on the micron/nanometre scale: (1) controlled, but not random (*e.g.* electrophoresis,[12] thermophoresis[13–16]), and (2) random, but not controlled (*e.g.* Brownian motion, and powered random walk, which we will discuss in more details later). Our objective is to combine both properties to achieve macroscopic control over locally random walks—sometimes called *powered* random walks—of synthetic self-propelled micro/nano-motors. In the past two years, our research groups have successfully observed phototaxis and quorum sensing of silver-containing microspheres,[17] emergence phenomenon of illuminated silver chloride particles,[18] and reversible particle packing reminiscent to phagocytosis. We have also observed predator–prey phenomena,[18] where one particle during movement preferentially seeks another particle, as one might see with a fox and a rabbit. How do these events happen? What are the physics describing our findings? Do our observations and models have any impact on actual biological events?

In this Perspective we describe the motion of micro/nano-scale particles that produce macroscopically controlled order, starting from the locally random movement of the individual particles. In section 2 we summarize the development of micro/nano-scale autonomous motors to date. This is the platform upon which we designed our non-biological motors, which have transport behavior that mimics biological systems, including chemotaxis and phototaxis. In section 3 we discuss the use of chemotaxis and phototaxis to achieve the control of global directionality in artificial micro/nano-motors, while maintaining the local randomness. Design principles for such locally random and globally directional systems are suggested where the interaction between the powering mechanism and the directing method is emphasized. The experimental observations are compared with their biological counterparts. Other bio-mimetic artificial systems (*e.g.* predator–prey) are also discussed. Section 4 concludes the point of this paper and suggests a direction of future research.

2. Powered random motion—autonomous micro/nano-motors

In scaling down to the low Reynolds number systems (denoted as the ratio of inertial forces to viscous forces),[19,20] the motion of an object is dominated by viscous forces rather than by inertia. A small-scale object encounters much stronger viscous drag as it moves in the fluid. Brownian motion can no longer be ignored, as it becomes a major contributor in particle motion. An autonomous micro/nano-motor has to overcome the viscous drag to be able to propel itself in the fluid, and has to have enough power to make its movement significant compared with Brownian motion. A number of theoretical models have been published in guiding the design of such systems.[19,21–27] There are, however, limited ways to realize micro/nano-scale autonomous motions[28] experimentally. Below we summarize most of these.

Neetu Chaturvedi

Neetu Chaturvedi was born in Kanpur, India. She received her Bachelor of Technology (BTech) degree from the Indian Institute of Technology, Kanpur. She is currently working towards her PhD under the guidance of Prof. Darrell Velegol at the Pennsylvania State University. Her research interests include fabrication of colloidal assemblies and the investigation and development of their applications.

Ayusman Sen

Ayusman Sen was born in Calcutta, India and holds a PhD from the University of Chicago where he was first introduced to catalysis. Following a year of post-doctoral work at the California Institute of Technology, he joined the Chemistry Department of the Pennsylvania State University where is currently Professor. He is a Fellow of the American Association for the Advancement of Science. His research interests encompass catalysis, organometallic and polymer chemistry, and nanotechnology. He is the author of approximately 275 scientific publications and holds 23 patents. His pastime centers on gastronomical explorations.

2.1 Asymmetric mechanical method

Najafi and Golestanian[21] proposed a simple one-dimensional swimmer model that consists of three spheres linked by rigid rods, whose lengths can change between two values. They showed that with a periodic motion in a nonreciprocal fashion, which breaks the time-reversal symmetry as well as the translational symmetry, the model device can swim at low Reynolds number. A more complex system was designed by Dreyfus *et al.*,[29] where a linear chain ($\sim$30 μm) of 1-μm-diameter superparamagnetic colloids linked by several 107-nm-long double-stranded DNAs and attached to a red blood cell can act as a flexible artificial flagellum. The filament can be actuated by oscillating a transverse magnetic field, which induces a beating pattern that propels the structure and controls the velocity and direction of motion. Continual external input is required and further downscaling can be difficult due to increasing viscous drag. Another interesting millimetre-scale robot was made by Kim *et al.* in 2007, where heart cells are attached to a molded polydimethylsiloxane (PDMS) robot. As the heart cells beat in a culturing solution, the device with asymmetric PDMS legs resembles a walking movement.

2.2 Surface tension

A well-studied example of a motor driven by surface tension is the camphor boat, on the scale of millimetres. A camphor boat propels itself on the surface of water as it dissolves asymmetrically and lowers the surface tension of the air–water interface.[30] This gave inspiration to the design of a variety of amphiphilic polymer gel swimmers from the millimetre–centimetre scale[31] to submillimeter[32] and micron scale,[33,34] which release water-soluble organic solvents to lower the surface tension at the air–water interface and self-propel in random directions. In this motor design, the gel swimmers need to be placed on the air–water interface and the volume of the swollen gel limits the length of the movement and downscaling in size becomes impractical. A more recent work[35] makes use of the Marangoni effect[36] by converting light into thermal energy, which in turn induces an interfacial tension gradient. A light absorbing material is placed at the rear part of a centimetre-scale object, which when illuminated, is propelled in the direction of the non-illuminated end since the heating effect results in lower surface tension.

2.3 Bubble propulsion

Remember the pop-pop boat? Air sealed in tubes underwater is released by heating, and bubbles pop out to propel the boat. A millimetre-scale ''pop-pop boat'' was designed by Dijkink and Prosperetti *et al.*[37] in 2006 where a sound field was used to release the bubbles. Further scaling down using the same technique is not feasible due to the limited gas volume. In 2005, Vicario and Feringa *et al.*[38] used a synthetic catalase mimic tethered on a microparticle to produce oxygen (O_2) from hydrogen peroxide (H_2O_2) and propel the particle. Later, Pantarotto and Feringa *et al.* immobilized a series of enzymes on a carbon nanotube to produce O_2 bubbles and propel the nanotube. In detail, glucose oxidase converts glucose to make H_2O_2, which is then decomposed by catalase to water (H_2O) and O_2.[39] At larger scales, bubble propulsion can work by inertia; at the micro-scale or smaller, surface tension and viscous effects will dominate.

2.4 Polymerization

In 1999, Cameron *et al.*[40] made self-propelled polystyrene beads by immobilizing ActA protein on the surface, which catalyzes actin polymerization and drives the bead to move at a speed of about 0.01–0.15 μm s^{-1} as it trails an actin filament tail, in resemblance to the generation of motile force at the leading edge of lamellipodia and filopodia. This is the only polymerization driven micro-motor reported so far, because polymerization usually requires strict control of conditions.

2.5 Catalytic self-electrophoresis

In 2002, Ismagilov and Whitesides[41] reported a centimetre-scale PDMS plate that propels itself by catalytically decomposing H_2O_2 with a fixed piece of Pt. Oxygen bubbles form at Pt and keep the plate moving for several days. In 2003, Paxton *et al.*[42–45] tried shrinking down the Pt-PDMS boat to submicron size PtAu rods by templated electrodeposition. They found that the 2-μm-long 370-nm-wide PtAu rods moved just as well even though bubbles were not seen coming out from the Pt segment. Further, the PtAu rods moved with Pt-end forward, a direction that was exactly opposite of that observed by Whitesides in their macroscale system. It was then they realized that bubble propulsion does not work for this specific model in the low Reynolds number system and a new mechanism was sought. After a few tentative hypotheses, the electrokinetic mechanism was found to be most convincing.[44,45] The mechanism states that Pt oxidizes H_2O_2 to produce H^+ and O_2 while Au consumes H^+ and reduces H_2O_2 to H_2O. In doing this, the PtAu rod generates its own electric field and moves relative to the surrounding fluid as a result of the ion flux (Fig. 1).

A variety of catalytic self-electrophoretic colloidal motors and micro-pumps have since then been designed.[4,46,47] For example, Ibele and Sen *et al.*[48] in 2007 reported the use of hydrazine (N_2H_4) as a fuel for PtAu micro-pumps; Wang *et al.* further found out that the use of mixed H_2O_2–N_2H_4 fuels greatly increased the movement speed.[4] Mano and Heller[49] made a self-propelled carbon fiber by immobilizing two sets of enzymes on the two ends of the fiber, one oxidizing glucose and the other reducing oxygen, to furnish an ion flow through

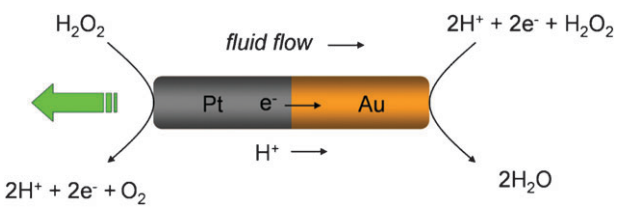

Fig. 1 A schematic illustrating self-electrophoresis. Hydrogen peroxide is oxidized to generate protons in solution and electrons in the wire on the platinum end. The protons and electrons are then consumed with the reduction of hydrogen peroxide on the gold end. The resulting ion flux induces motion of the particle relative to the fluid, propelling the particle toward the platinum end with respect to the stationary fluid.[28]

the carbon fiber. The asymmetric placement of redox catalysts is an important design element in self-electrophoretic micro/nano-motors.

Some of our findings echo reports from the 1960s. In order to coat metals with polymeric resin (latex), Steinbrecher and Hall described a method for effecting auto-electrophoresis of the particles toward the metal surface.[50] That is, their electrodeposition required no impressed current. This electroless deposition method, described in more detail as chemiphoresis in a later publication by Prieve and coworkers,[51] provides a method for very uniform coatings, since the presence of the coating tends to diminish the tendency to add new a coating. It is a negative feedback loop. While the physics of our own process has been known in principle for 40 years, the enhanced materials synthesis capabilities through advances in chemistry and nanoscience has enabled new control over self-propelled motors. Since our motors combine elements of directed motion (auto-electrophoresis, auto-diffusiophoresis) with random motion (Brownian translation and rotation), this research enables studies of emergent/collective behavior, and thus model biology.

2.6 Self-thermophoresis

Thermophoresis, also called the Soret effect, is the transport of mass in a temperature gradient.[52–56] Soret effects both up or down the temperature gradient have been observed.[57] A model colloidal motor that is capable of generating and maintaining a thermal gradient across the surface of the motor might consist of a Janus particle composed of two faces possessing different light-absorbing abilities. Under a global illumination, the particle develops a temperature gradient in its vicinity and the thermal diffusion of the fluid may result in movement of the particle. This is indeed very similar to the previously mentioned light-to-work surface tension-driven motor[35] except that a different mechanism is proposed. No experimental results have been published with regard to self-thermophoresis. It remains to be seen whether a micro/nano-scale thermophoretic motor is realizable, and if the answer is yes, whether the Soret effect or the Marangoni effect is dominant.

2.7 Self-diffusiophoresis[14,58,59]

Diffusiophoresis usually refers to the movement of a particle by the electric field and pressure field set up by the differential diffusion of specific cations and anions (Fig. 2). The phenomenon is actually more common than the unfamiliar scientific term suggests. For example, if you put a drop of water containing small tracer particles on a glass slide, after about 5 min you will see circular exclusion zones in a few random areas. More specifically, if you make a scratch on a glass surface and spread some water with small tracer particles on top, you will see the tracer particles racing away from or towards the scratch at a remarkable speed (10s of μm s^{-1}). The direction of the flow depends on the type of glass and the sign of charge that the tracer particle carries. This happens because the bulk of the glass under the surface contains significantly more alkali ions, typically sodium. The scratch exposes the bulk and ions leach out to form a concentration gradient. Benjamin and Mallouk *et al.*[60] first reported a similar phenomenon in 2002

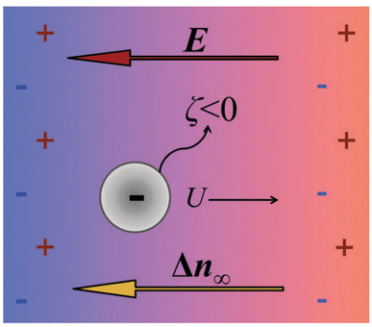

Fig. 2 Schematic of diffusiophoresis. Differential ion diffusion causes temporary electric field (E), within which a particle moves with a velocity U depending on its ζ-potential. At the same time, the chemical concentration gradient (Δn_∞) drives the particle movement in the direction of lower chemical concentration (yellow arrow points towards higher concentration).

where they found surprisingly large exclusion zones around some dust particles (Fig. 3), which cannot be explained by electrostatic repulsion due to the small Debye length of the system. It is likely that they observed a diffusiophoretic phenomenon. Ibele *et al.* further observed that some small pieces of fresh glass dust might even become motile boats, propelling themselves as they leach out ions, and repelling the tracer particles at the same time to clear out their own paths (Fig. 4). Here the ions are generated by the particle itself, which is the basic principle in designing a self-diffusiophoretic machine. Asymmetry is not required for small particles because either the heterogeneity of the particle or the random fluctuation of ions plus thermal motion is sufficient in providing the temporary directionality.

It is not necessary to use a salt solution reservoir to furnish a self-diffusiophoretic motor. Golestanian *et al.*[61] proposed a theoretical model where the motion of a colloidal sphere is driven by an asymmetric distribution of reaction products. Howse, Jones and Golestanian *et al.*[22] further confirmed the model with experiments using polystyrene microspheres coated on one side with Pt to catalyze the decomposition of H_2O_2. As more molecules of reaction products are produced than are consumed, and the catalyst is asymmetrically distributed, the sphere is propelled at speeds of 0–3 μm s^{-1}. Our own research reveals that silver-coated colloidal spheres (colloid–Ag Janus particle), when placed in dilute H_2O_2 solution, release Ag^+ and OOH^- ions asymmetrically upon the irradiation of ultraviolet light and move at a speed of

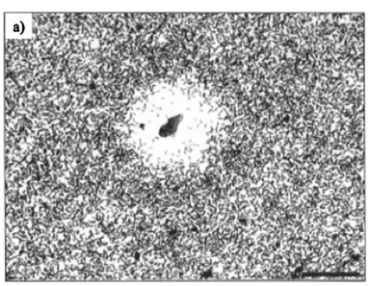

Fig. 3 A dust particle repels mercaptoethylsulfonic acid (MESA)-derivatized particles on MESA-derivatized surfaces. Scale bar = 50 μm.

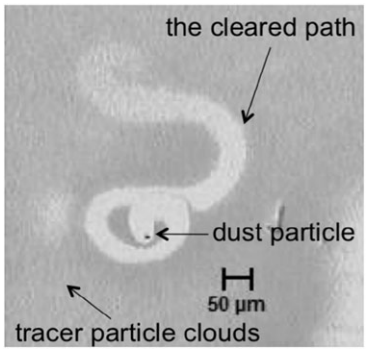

Fig. 4 A dust particle cuts through the clouds of tracer particles as it moves.

about 2 μm s^{-1}, because Ag^+ diffuses 5 times faster than OOH^- (Fig. 5).

We also fabricated micron-sized colloidal heterodoublets of Ag–amidine polystyrene latex (PSL), Ag–sulfated-PSL and Ag–silica (Fig. 6). These fabrication methods provide a simple, quick and inexpensive approach to the assembly of synthetic motors from colloidal particles. While the Ag–amidine PSL heterodoublet is fabricated utilizing the attractive electrostatic interaction between the constituent particles, the Ag–sulfated-PSL and Ag–silica heterodoublets are fabricated using the salting-out–quenching–fusing technique (SQF).[62–64] The heterodoublets moved at approximately 1–2 body lengths per second in 0.25% H_2O_2 under UV (Fig. 7).

The velocity of a particle undergoing diffusiophoresis is the sum of a diffusiophoretic component (eqn (1)) and an electroosmotic component due to the substrate. The diffusiophoretic velocity of a charged particle in a uniform concentration gradient field is given by

$$U_{dp} = \frac{\varepsilon kT}{Ze\eta}\left[\left(\frac{D_+ - D_-}{D_+ + D_-}\right)\zeta_p - \frac{2kT}{Ze}ln(1-\gamma^2)\right]\frac{\Delta n}{n_0} \qquad (1)$$

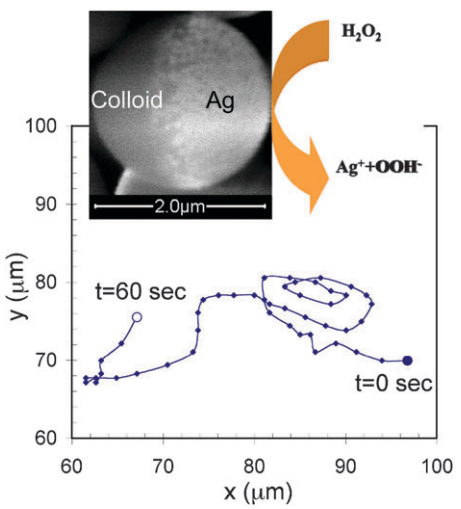

Fig. 5 The movement path of a SiO_2–Ag Janus particle in 0.5% H_2O_2 under ultraviolet irradiation, observed with an optical microscope. Each data point is 1 s apart. The inset shows a scanning electron microscope image of a sulfated polystyrene sphere coated half with silver.

where D_+ and D_- are the diffusion coefficients of the cation and anion, respectively, Z is the absolute value of the valence of the ions, e is the charge of a proton, k is the Boltzmann constant, T is the absolute temperature, ε is the dielectric permittivity of the solution, η is the viscosity of the solution, ζ_p is the zeta potential of the particle, $\gamma = \tanh(Ze\zeta_p/4kT)$, n_0 is the concentration of ions at the particle surface, and Δn is their concentration gradient. The electroosmotic velocity is given by a similar equation, with the particle zeta potential replaced by the wall zeta potential. Of course, the particle is not in a uniform concentration gradient, since it is in fact creating its own concentration gradient which will have a more complex geometry. However, the variables in these equations are the same as those that will impact the particle's speed. Therefore, the equations give order-of-magnitude estimates of particle velocities, providing guidance to a researcher aiming to design a system with a given velocity.

It should be noted that structural asymmetry is not always required for a diffusiophoretic motor. Golestanian[65] calculated in a recent publication that symmetric objects within a certain hydrodynamic regime can be propelled by self-diffusiophoresis as a result of density fluctuation. We also observed that spherical 1μm Ag colloids in H_2O_2 move under UV light, possibly also due to the inherent heterogenety on the particle surface.

2.8 Osmotic propulsion

Not only can ionic species induce motion, the diffusion of neutral species can also cause particle motion by means of osmotic propulsion.[27] This works by the creation of an osmotic pressure imbalance on the motor, orginating from nonequilibrium concentration distribution of bath particles, causing the motor to move. Córdova-Figueroa and Brady[27] demonstrated theoretically that this could be used to propel nano-objects. The finding adds to our current tools in designing micro/nano-motors and the existence of osmotic-pressure-induced motion might in fact be much wider than realized.

The characteristics of the above-mentioned micro/nano-motors are that they are autonomous, self-propelled, and perform random walk, even though instantaneous directionality might exist (*e.g.* the PtAu rods move with the Pt end forward). In this respect, they can be treated as a *powered Brownian motion* with longer step length and smaller rotational diffusion coefficient. In fact, we have shown that for a particle having a speed (U) and a rotational diffusion coefficient (D_r), the powered diffusion coefficient is $D^* = U^2D_r$. For practical applications, mechanisms to control the directionality of motion are required.

3. Control of the random motion

Control of directionality at the micro/nano-scale can easily be done by using light, electric field,[12] magnetic field,[66,67] thermo-gradient,[15,16] or electrolyte gradient.[33,37,38] This controlled directionality comes with at least some sacrifice of randomness.

The scratched glass experiment is a simple example of controlling the direction of movements by diffusiophoresis. Thanks to Anderson,[14] our understanding toward diffusiophoresis

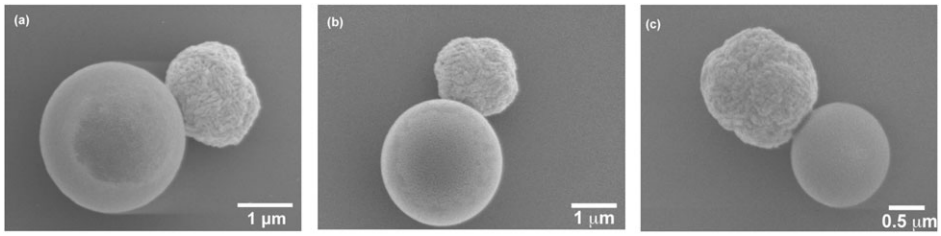

Fig. 6 Scanning electron microscopy image of doublets of (a) 2.5μm amidine-functionalized PSL particle and 1.5 μm silver particle, (b) 2.4 μm sulfate-functionalized PSL particle and 1.5 μm silver particle, and (c) 1.54 μm silica particle and 1.5 μm silver particle.

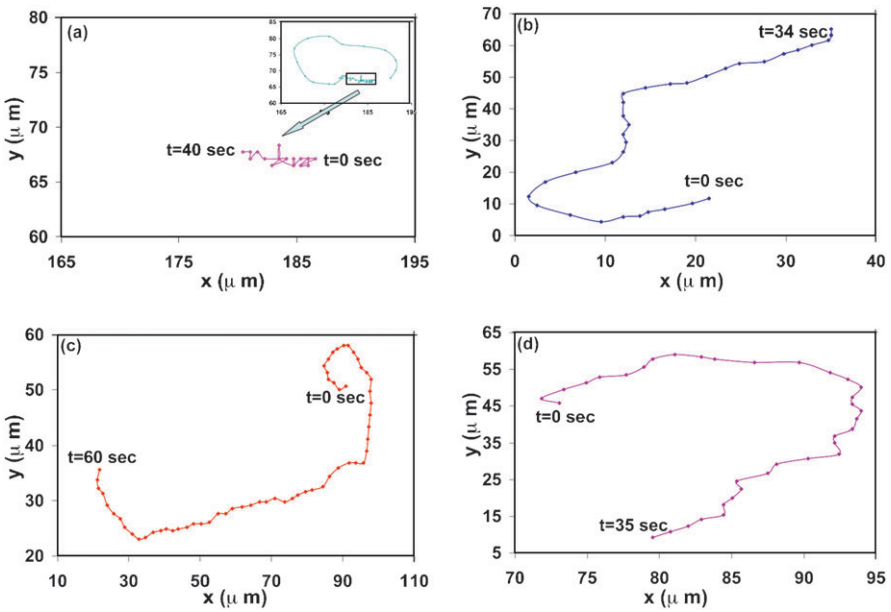

Fig. 7 Paths of colloidal doublets in 0.25% H_2O_2, observed with an optical microscope and tracked using Physvis. (a) Silver–amidine PSL doublet with no UV irradiation; Inset shows the path of the same doublet before and after UV irradiation, (b) Silver–amidine PSL doublet upon UV irradiation, (c) Silver–sulfated-PSL doublet upon UV irradiation, (d) Silver—silica doublet upon UV irradiation.

has enabled us to construct a diffusiophoretic system with precise control by selecting the ion species, adjusting the ionic strength, and coupling the ζ-potentials of the particle and underlying surface materials. Control of directionality on the PtAu catalytic colloidal rods has also been done by means of magnetic field. Kline *et al.*[2] were able to restrict the directionality of a catalytic metallic nano-rods down to 1-dimension by placing the nickel striped PtAu rods in a magnetic field, which aligns the rods by orienting their net magnetic moments. Dhar *et al.*[3] further used heterogeneous magnetic fields to navigate nickel striped colloidal rods or rods that are functionalized with iron oxides (Fe_3O_4) nano-particles embedded in poly-pyrrole. These methods gain directionality by eliminating or reducing the intrinsically random orientation of the micro/nano-movers.

On the contrary, directing a group of motors while maintaining the randomness in each motor can be a more challenging task. One might use external signals, in addition to the self-propulsion system, with the aim of overlaying directionality on top of the random motion of the motors. However, there is a distinction between controlling the motion of the motors at the individual level, or at the collective level. For example, if the directionality of the individual motors is biased by an imposed magnetic field, the particles will all tend to move in a particular direction. Alternatively, if the individual motion of the particles generates a field that, only when a number of particles participate, is significant enough to give each participant a bias to direct their motion, which in turn alters the field. The latter provides a lot more possibilities in intelligent artificial systems design. A similar idea was suggested by Golestanian in his recent publication.[65]

3.1 Chemotaxis

Tactic responses of microorganisms to chemicals or light are important in a wide variety of biological processes involving directed movement of cells. Movement of an organism in response to external directional cues by moving towards or away from a particular source was first discovered by Engelmann in the 1880s.[7–9] He identified phototactic, aerotactic and chemotactic behavior in some bacteria, documenting their aggregation in areas that are favorable to them because of light, oxygen or other chemicals, respectively. Since then, chemotaxis has been studied extensively both in prokaryotes and eukaryotes. Chemotaxis is the fundamental mechanism by which immune cells locate the inflammatory sites and is

essential to wound healing.[68–73] It is also involved in the metastasis of cancer cells where target organs secrete binding ligands that are detected by the chemokine receptor of the cancer cell.[74,75] As for bacteria, chemotaxis is the primary mechanism that enables them to look for food and escape from toxins. Bacteria use spatial sensing and temporal sensing[68,76–79] to respond to external cues. Temporal sensing is particularly useful for small bacteria that are not capable of distinguishing chemical concentration difference across their short body lengths. In a temporal sensing mode, bacteria swim in random directions in a manner that consists of straight run and reorienting tumbling. It is the ratio of straight run to tumbling that small bacteria adjust to select their direction in a chemical gradient, rather than directly adjusting the orientation. When the concentration of chemo-attractant increases, bacteria tumble less and as a result, move straighter ahead; when the concentration of chemoattractant decreases, bacteria tumble more frequently in an effort to reorient themselves. The biased selection of motion results in the overall chemotactic response. The current biochemical research has no doubt led to a deeper understanding at the molecular level of bacterial chemotaxis, which involves complex signal transduction systems.[10] The question left to chemists and physicists is this: can we incorporate such "bacterial intelligence" into self-motile micro/nano-particles without introducing the complex molecular biology mechanism?

We wondered whether PtAu rods are able to gain orientational bias in a concentration gradient of their fuel—H_2O_2. In other words, will they be able to sense the concentration difference of H_2O_2 and take actions accordingly? As was mentioned previously, PtAu rods swim autonomously and randomly when placed in a uniform concentration of H_2O_2 solution by self-electrophoresis. When the chemical fuel is distributed inhomogeneously such that it has a gradient, homogeneity could be broken and the rods may acquire a subtle bias, which can be measured cumulatively as the population of rods redistribute spatially according to the concentration gradient of H_2O_2. The bias may function *via* the rod speed–H_2O_2 concentration relationship, where higher fuel concentration affords faster swimming. The diffusion coefficient of PtAu rods increases consistently with H_2O_2 concentration up to 10% (Fig. 8). We observed the accumulation of rods in two sets of experiments.[80] In the first case, an agarose gel was used to create the concentration gradient of H_2O_2. The gel was pre-soaked in 30% H_2O_2 and then placed in a solution of uniform PtAu rod concentration in deionized water. As the H_2O_2 slowly diffused out, the PtAu rods closer to the gel started migrating towards the gel at a marginal yet positive speed. A difference was seen after about 10 h when the rods became denser near the gel (Fig. 9). Control experiments showed that non-active polystyrene spheres did not migrate towards the H_2O_2 source. In the second experiment, four capillaries containing different concentrations of H_2O_2 were placed in a solution of PtAu rods in deionized water. In as short as 1 h, the capillary containing the highest concentration of H_2O_2 showed the highest concentration of rods (Fig. 10). It should be noted that the above observations are complicated by gradient-induced fluid flow patterns that cause particles to move towards or away from the gel, depending on their depth

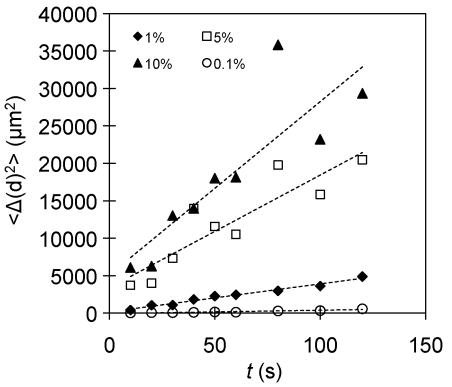

Fig. 8 The mean square of displacement of PtAu rods in various H_2O_2 concentrations.

in the fluid layer. This aspect of particle movement is still under active investigation.

The phenomena described above was predicted qualitatively and even quantitatively using Brownian dynamics simulations (BDS).[81] BDS are often used to evaluate the movement of particles having complex transport dynamics over times.[81] BDS allows for analysis of convective movements (total velocity U) like electrophoresis, gravitational settling, or magnetically forced transport, or any auto-transport, as well as diffusive movements like Brownian translation and Brownian rotation. The essence of the method is to take account for the movement of all particles, either individually in the simplest case or collectively in more accurate work, in nearly-differential time steps (Δt).

$$x(t + \Delta t) = x(t) + U\Delta t + \Delta x(\Delta t) \qquad (2)$$

The simulation marches on in time, adjusting the new speed and orientation with each time step. The last term in eqn (2) is due to Ermak and McCammon,[82] who found that gradients in diffusion coefficients lead to an effective directed motion of the particles. In our simulations we do not need this term for

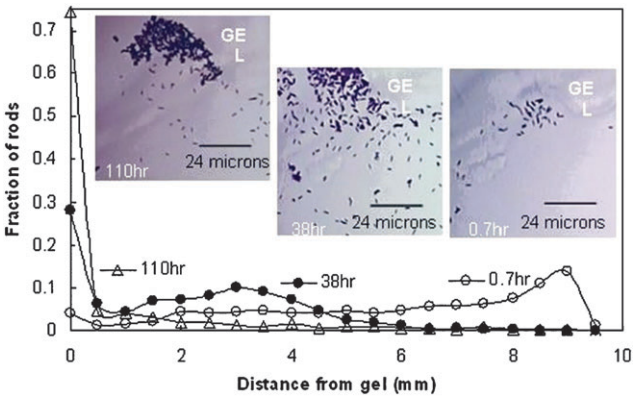

Fig. 9 The changing distribution of PtAu rods in an H_2O_2 concentration gradient. The gel (soaked in 30% H_2O_2) appears in the upper part. The images were taken at 0.7 h, 38 h, and 110 h. The fraction of rods was evaluated by dividing the number of rods in a frame at a certain distance by the total number of rods summed up from the frames at all the distances. Insets show the change in population of PtAu rods near the gel, visualized under bright field inverse microscopy.[80]

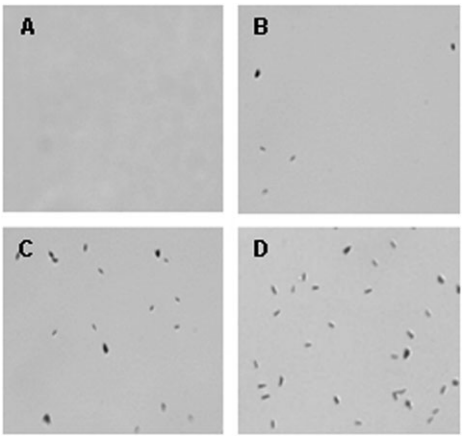

Fig. 10 Capillary experiments showing chemotaxis from bulk solution into the capillary. The capillaries initially containing (A) 0% H_2O_2, (B) 0.5% H_2O_2, (C) 1% H_2O_2, (D) 10% H_2O_2 seen after 1 h. An increase in the population of rods occurred with increasing initial H_2O_2 concentration. The images were taken at 40× magnification. Brightness and contrast were adjusted and cropping was done by Microsoft Office Picture Manager.[80]

gradients of actual diffusion coefficients. However, it is interesting that due to the Brownian rotation of the particles, which we also account for step-by-step, we obtain a powered diffusion coefficient $D^* = U^2/D_r$ that gives essentially the same physics as Ermak and McCammon found for Brownian diffusion. The details of our simulations are given elsewhere.[80]

So how do we understand the phenomenon in a simple picture of physics? Without a temporary memory algorithm as in bacteria, PtAu rods chemotax by differential powered diffusion, combining both electrokinetic translation and the Brownian rotation. The rods move either up or down the gradient for the same finite amount of time (τ), which is controlled by the rotational diffusion coefficient (D_r). When they move up the gradient, they speed up due to increasing H_2O_2 concentration; whereas when they move down the gradient, they slow down. This poses a slight tendency for the ensemble of rods to move up the gradient.

In bacterial chemotaxis, the ratio of straight walk to tumbling is increased by reducing the tumbling frequency; whereas in the PtAu rod chemotaxis, the ratio of straight walk to the rotational diffusion is regulated by the change of step length. But does the rotational movement remain completely steady throughout the process? In other words, does the rod reorient slower when it senses higher H_2O_2 concentration, just like bacteria do when they sense more food? Even though the direct measurement in an H_2O_2 gradient was inconclusive, the measurement in homogeneous H_2O_2 solutions did show a slight decrease in the rotational diffusion coefficient of PtAu rods with increasing fuel concentration (Fig. 11, the measurement was done by MatLab, which measures the change of rod orientation over time), which was not seen if the rods were non-active (Au rods in Fig. 11). The experiment setups, however, are subject to strong hydrodynamic flows originating from the mixing of two fluids. We are currently attempting to distinguish the possible chemotactic motion from the fluidic flow.

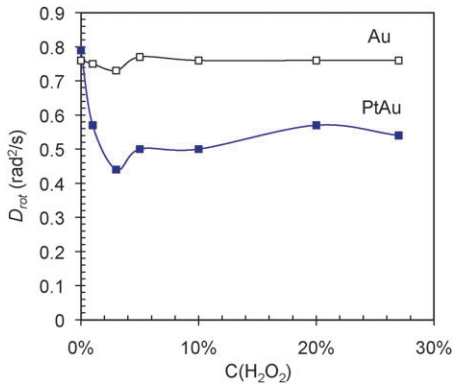

Fig. 11 The rotational diffusion coefficient of PtAu rods (active) and Au rods (non-active) in homogeneous concentrations of H_2O_2.

Such stochastic bias was recognized on eukaryotic cells such as neutrophils[83,84] and *Dictyostelium*[11] as well. The current research is uncovering more and more organisms that adopt a stochastic model. Prior to 2007, it was generally believed that *Dictyostelium* chemotaxes by making new pseudopods at locations of higher chemoattractant concentration. However, it was recently discovered by Andrew and Insall[11] that the chemotaxis of *Dictyostelium* in a shallow gradient is mediated independently of PtdIns 3-kinase, by biased choices between random protrusions, *i.e.*, by regulating the survival and retraction of existing pseudopods rather than making new ones at more correct directions. The generation of new pseudopods is random with respect to both timing and direction. Even in a polarization mechanism,[68,84–86] where the cell fronts are constantly protruding and retracting pseudopods and orient according to the chemical gradient, the cells chemotax in the correct direction, consistently but not perfectly.[87]

3.2 Phototaxis

Some cells and organisms can be responsive to light and make appropriate adjustments of their orientations accordingly. The oriented movement of a locomotive organism with respect to the direction of light is called phototaxis. The movement can be either towards a light source (positive phototaxis), or away from the source (negative). Engelmann discovered the first example of phototaxis by showing that bacterial strain *B. photometricum* responds to infrared and visible light by accumulating in distinct bands.[8] Photosynthetic pigments or photoreceptor proteins present in the bacteria absorb the light, which then generates a signal *via* electron transport, feeding into a canonical chemotaxis signal transduction pathway and thus responding to external stimuli. The cellular apparatus which mediates the response consists of a receptor, a transducer, and an effector, each of which may be a complex, multi-component system.[88]

We experimentally achieved phototaxis with our colloid–Ag micro-motors—that is, with non-biological rods—by creating a UV light gradient.[17] As we mentioned above, the Ag-coated particle (diameter 2 μm) in dilute H_2O_2 (usually below 0.5%) produces Ag^+ and OOH^- upon UV irradiation and is moved by the self-generated diffusiophoretic field. Here UV acts as the only external cue to initiate the reaction, thus only particles that are illuminated by UV release ions. As a result, a

non-uniform UV field can set up a macroscopic ion gradient with most concentrated ions in the best illuminated area. This leads to a mass transport of particles by diffusiophoresis. We have actually observed a negative phototaxis with the colloid–Ag Janus particles (Fig. 12), where they wander away from the circular UV spot (diameter 600 μm). The way they escape from the UV light is highly random, due to the interaction of the localized ion gradient around the particle and the longer-range gradient produced by the ensemble of particles collectively. It is interesting to see a sequence of effects in our simple nano-motor systems, when the motion is due to UV light. Collections of particles move away from the UV light, due to the concentration gradient set up collectively by the particles. Then, the same collections of particles move back into the UV light, due to the thermal gradient that forms. The interaction between these different mechanisms can produce significant complexity, which can look almost life-like when watched over time.

The event resembles quorum sensing,[89–91] in that a concentration threshold exists for the event to happen. Quorum sensing is a strategy developed by small organisms, including bacteria and social insects, to overcome their size limit by social coordination. The individual contribution facilitates the message delivery to the whole community. Similarly, the ion gradient generated by individual colloid–Ag Janus particles is not enough to induce the phototactic behavior; it is the ensemble of the particles working collectively to achieve the macroscopic order. The critical concentration of particle is about 1×10^6 mL^{-1} under our conditions. A higher particle concentration greatly improves the phototactic effect, in that better defined edge and faster formation of patterns were observed.

In our own case, Brownian dynamics simulations, described previously, are especially useful since the velocity of the ith motor (U_i) depends on the local concentration of fuel, which in turn depends upon the catalytic reactions of all the motors in the region. Thus, there is a feedback loop that leads to the complex emergent behavior.

A BDS model was used with algorithms similar to that used in chemotaxis of PtAu rods. The particles were treated as point sources of ions. A dimensionless time $\tau = t(D_+ + D_-)/2r_0^2$ was used. The model predicted that a more negative ζ-potential would result in better defined patterns (Fig. 13 right column. ζ_p is the particle ζ-potential, about -30 mV for most of our particles; ζ_w is the underlying surface ζ-potential, which is -60 mV.[92]). Notice that in the model, small clusters are predicted to appear as early as 60 min ($\tau = 40$). The non-random autonomous movement of the particles is driven, at the level of the individual particle, by the chemical reaction, which produces an electrolyte gradient, which in turn acts on the particle and substrate (since they each have a finite ζ-potential), causing diffusiophoresis. Macroscopically, diffusiophoresis causes phototaxis of the system.

Similar experimental phenomena were observed with colloidal heterodoublets. The colloidal heterodoublets are fabricated in a simple, quick and inexpensive way, using particles of various materials compositions. Each heterodoublet is an independent entity that can perform self-propelled movement. Along with the heterodoublets, the solution also contains uncoupled singlets and some higher order aggregates. The pattern

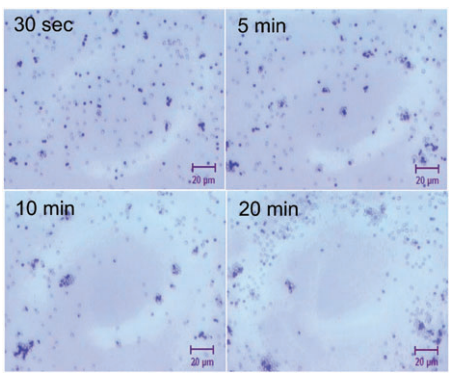

Fig. 12 Time-lapse images show the phototactic process of SiO_2–Ag particles in 0.5% H_2O_2 under the irradiation of a circular ultraviolet light. The contrast and sharpness were enhanced by Photoshop.

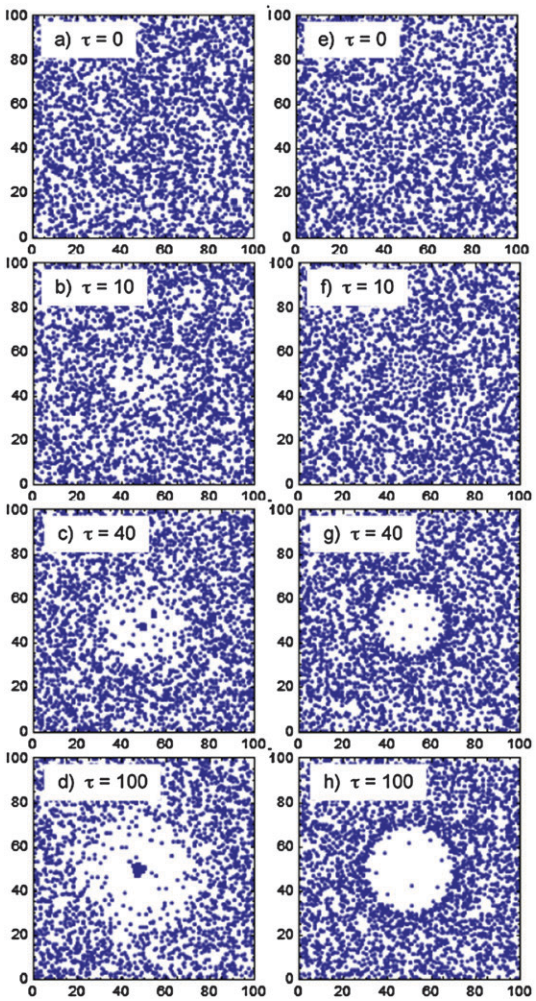

Fig. 13 Brownian dynamics simulation results. Images (a)–(d) are for $\zeta_p - \zeta_w = +25$ mV and (e)–(h) are for $\zeta_p - \zeta_w = -25$ mV. $\tau = 1$ corresponds to a time of 90 s. Each unit of length is $0.1 \times r_0 = 0.03$ mm. The number of particles is set to 3000. The particle size is taken as $2a = 2$ μm, although the particle size does not impact the calculation since we assume thin electric double layers. The variable $\tau = t(D_+ + D_-)/2r_0^2$, where r_0 is the laser spot radius 0.3 mm.

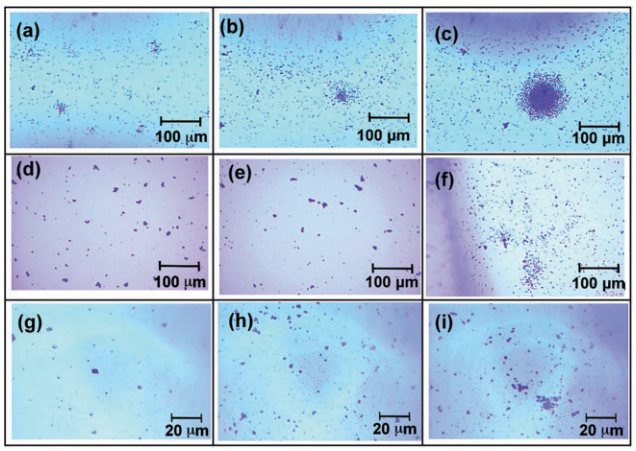

Fig. 14 Time-lapse optical microscope images of heterodoublets showing their phototactic process in 0.25% H_2O_2 under UV illumination. (a, b, c) Silver–amidine PSL doublets and higher order aggregates (a) 0 min, (b) 30 min, (c) 100 min; (d, e, f) Silver–sulfate PSL doublets and higher order aggregates (d) 0 min, (e) 10 min, (f) 100 min; (g, h, i) Silver–silica doublets and higher order aggregates (g) 5 min, (h) 50 min, (i) 80 min.

formation of the heterodoublets over long time in the presence of H_2O_2 and UV light is governed by diffusiophoresis, as well as by thermal diffusion. While Ag–amidine PSL doublets formed a thick cluster of particles at the center of UV region with a relatively deficient region of particles around it, Ag–sulfated-PSL and Ag–silica doublets initially moved away from the center then formed smaller clusters at the center at longer times (Fig. 14). The motion back to the center arises since the metal particles absorb the UV light, causing the local solution to heat up, and therefore increasing the local diffusion coefficient. By the Ermak and McCammon term of the BDS, the particles tend to move toward this region of higher diffusion coefficient.

An interesting observation was the "Pac-Man" effect seen with Ag colloidal particles, as shown in Fig. 15, where a bigger particle engulfs any smaller particle in its vicinity. These catalytic particles formed bigger structures in the presence of H_2O_2 and UV radiation, due to the ion release, by attracting nearby particles in the solution. This is reminiscent to the slime mold convergence, where unicellular slime mold *Dictyostelium* amoeba, when stressed, secretes cyclic adenosine monophosphate (cAMP) as a chemoattractant to nearby amoebae, which respond by secreting additional cAMP to amplify the signal, so that all amoebae start moving up the global cAMP gradient to form colonies and assemble multi-cellular fruiting bodies.[68,93] In our systems, the ions released from each individual particle results in diffusiophoretic response from nearby particles which, when close enough, swim up the concentration gradient. More ions are released as the structure grows bigger. The Pac-Man effect is different from thermodynamically-driven Ostwald ripening, because it is reversible in that removing UV light results in re-dispersion of the aggregated structure.

The colloid–Ag systems do have some limitations. The bubbles produced prevent the formation of nice, clean patterns in some cases, and patterning of the colloidal particles using a photo-mask was complicated for the same reason. Moreover, the systems are dissipative. They stop working when the silver is completely consumed. In this sense, the heterdoublets offer a bigger fuel-pack and longer lifetime. What is important is that they provide a prototype for designing an artificial phototactic system and a simplified quorum sensing model.

3.3 Predator–prey

We have seen the intra-particle Pac-Man effect of Ag colloidal particles and heterodoublets in the example of non-biological phototaxis. Inter-particle phagocytosis-like behavior was also reported recently.[18] Micron-sized silica particles, when mixed with silver chloride (AgCl) micro-particles, actively seek out the AgCl particles under UV illumination. As a result, the silica particles engulf the AgCl particles by surrounding them (Fig. 16). This motion originates from the photodecomposition of AgCl and the release of ions into the solution, which causes electrophoretic and electroosmotic flows around the AgCl particles, to which the silica tracer particles respond.

Similar particle interactions are seen between colloidal-sized Titania (TiO_2) particles and other inert colloids, where TiO_2 reversibly repels or attracts other particles under UV illumination as a result of TiO_2's photoactivity.[94] The principle is relatively straightforward: One just needs a field generated by particle A to be detected by particle B, which can interact with or be influenced by the said field. In the example shown in Fig. 16, the field is a chemical gradient produced by AgCl under UV light, the interaction is a balance between the electrophoretic force involving the charge of the silica particle, and the electroosmotic force related to the charge of the underlying material.

3.4 Particle communication

One essential aspect of living organisms is that they are able to communicate with each other through complex chemical signaling processes. This allows cells or small living entities, *e.g.* insects, to cooperate and carry out complex functions, giving collective behavior. Quorum sensing is one example of biological communication *via* chemical signals. This was seen in our colloid–Ag phototaxis systems in that individual particles communicate by responding to the global chemical gradient generated collectively.

An interaction between the particle-generated electrolyte gradient and other charged tracer particles can further induce a predator–prey-like phenomenon, where the tracer particle chases the motor particle by catching up with the diffusiophoretic flow near the motor particle. The principle might appear simple, but has some resemblance to the way a neutrophil chases its bacterial prey by chemotaxing up gradients of formylated peptides released by the bacteria.[87]

Many other interesting particle communication systems can be designed using various mechanisms. One theoretical example is proposed by Usta and Balazs *et al.*,[95] where one polymeric micro-capsule signals to another and thereby initiates the motion of both. In particular, two capsules are placed on a homogeneous adhesive surface. A first capsule secretes nano-particles which chemisorb onto the substrate and modify the wetting properties of the surface. The adhesive

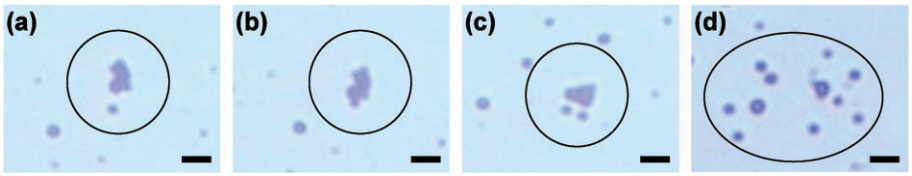

Fig. 15 Silver particles showing a ''Pac-Man'' effect in 0.25% H_2O_2 under UV irradiation. Images (a) and (b) are in the presence of UV light showing the bigger cluster engulfing a smaller particle, while images (c) and (d) are in the absence of UV light showing the disintegration of the bigger structure. (a) 0 s, (b) 1 s, (c) 10 s and (d) 30 s. UV light was removed at $t = 7$ s. Scale bar = 5 μm.

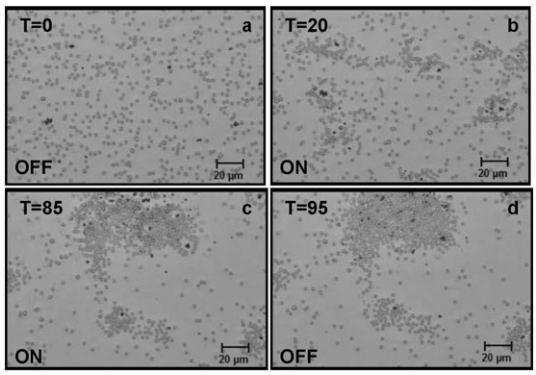

Fig. 16 Predator–prey behavior of two different particles. AgCl particles (darker objects) have been mixed with 2.34 μm silica spheres and placed in deionized water (a). When illuminated with UV light (b and c) the silica spheres actively seek out the AgCl particles and surround them. While the UV light is on, an exclusion zone is seen around the AgCl particles; this exclusion zone disappears when the UV light is turned off (d). Times in seconds are listed in the upper left hand corner. Status of the UV light is listed in the bottom left.[18]

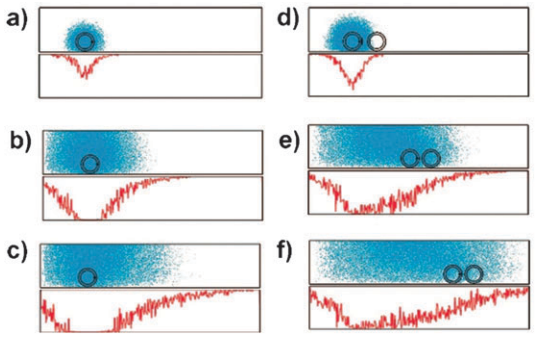

Fig. 17 Snapshots of a single capsule and two capsules on an adhesive substrate. The initial conditions are identical for both simulations. The signaling capsule releases nano-particles (in blue), which deposit on the surface and produce the adhesion profile shown in red. (a–c) Due to the symmetry of the adhesion profile, the single capsule remains stationary. (d–f) The target capsule sits on an asymmetric adhesion profile, which results in a net force driving the target capsule away from the signal capsule. Once the target capsule starts moving, it displaces the surrounding fluid, which drags the signaling capsule. Thus, the hydrodynamic interaction initiates motion of the signaling capsule, which is then sustained by the adhesion gradient.[95]

interaction between the capsules and the surface decreases with the fractional surface coverage of the nano-particles, therefore creates an adhesion gradient along the surface. A second capsule could then be driven by enthalpic forces to move from a less adhesive region to a more sticky region, and as it moves the fluid flow created thereof drags the signaling capsule (Fig. 17).

4. Conclusions and outlook

A catalytic nano-motor is a self-propelled, non-biological particle that gives random movement on local microscopic length scales. Macroscopic, external field-induced control of particle movement has long been available; commonly used examples include magnetic fields, electric fields, optical guides, and thermal gradients. The catalytic motors can also move with a macroscopic control that is *emergent*, either due to chemotaxis, phototaxis or thermotaxis. For our catalytic motor systems, there are two local driving forces that cause the random motion of the particles. (1) Each motor has a self-powered motion, due to auto-electrophoresis or auto-diffusiophoresis, for instance. There is a small amount of Brownian translation super-imposed upon this self-powered motion, but it is often negligible. (2) Brownian rotation changes the direction of each catalytic motor as it moves. In addition to these two local driving forces, there is a macroscopic driving force for the system, in the case of phototaxis, caused by the macroscopic ion gradient produced collectively by all the motors acting simultaneously. This interesting behavior—that the motors both produce the concentration gradients or electric fields, and are driven by them—is at the heart of our emergent systems, giving local randomness but macroscopic control.

These transport mechanisms give rise to the Pac-Man effect, predator–prey chasing, or quorum sensing. As a result, catalytic motors mimic biological systems in their transport phenomena, although the mechanisms for artificial motors are generally simpler than the mechanisms for bacteria for other biological systems.

Using a suite of techniques, we now have the ability to fabricate simple motors with metal, oxide, polymer, or other components. Although the physics of the catalytic motors is old (*e.g.* electrokinetics and Brownian dynamics simulations), the fabrication chemistry is new. The ability for our motors to autonomously take energy and information from their environment arises because of the design that goes into the motors: the materials that are used, the architecture between different components, their zeta potentials, and the catalyst–fuel combination. There are a number of knobs that we have at our disposal.

Our work is now leading to the concept of ''intelligent motors''. Intelligence requires that an object be able to anticipate and adapt. A simple form of anticipation is that

an object samples a region of space, and then selects whether to proceed. As humans we sample and select continually, and stochastic behaviors are seen in organisms ranging from bacteria to human beings.[96] Stochastic algorithms have also been used in artificial intelligence. And thus random sampling contributes to intelligence, in a way that deterministic motion cannot. We are working to enhance the abilities of our motors to sample and interact with their environment, to cause action. An additional component to the motors, which we are currently working on, is the development of a simple temporal memory. Memory might result, for instance, from a chemical capacitor, which could absorb/adsorb and release chemical components.

The idea is to learn from the nature and recreate biological functions using simple physics on artificial objects so that we can incorporate a certain degree of intelligence into non-biological micro/nano-bots. For example, upon pondering the process used by immune cells to locate an inflammatory site (chemotaxis), we might consider a design that enables an interaction between the exudates and the powering mechanism of the therapeutic nano-bot, which might prove more efficient for therapeutic purpose than the current concept of immobilizing a target-specific detector on the nano-bot.

Acknowledgements

The authors thank the National Science Foundation for funding this work through the Center for Nanoscale Science (MRSEC), NIRT grant # CTS0506967, CBET grant # 0651611. This publication was also supported by the Pennsylvania State University Materials Research Institute Nano Fabrication Network and the National Science Foundation Cooperative Agreement No. 0335765 (NNIN). We thank Thomas Mallouk, Vincent Crespi, Paul Lammert, Joseph McDermott, Shakuntala Sundararajan and Michael Ibele for stimulating discussions.

References

1 T. E. Mallouk and A. Sen, *Sci. Am.*, 2009, **300**, 72–77.
2 T. R. Kline, W. F. Paxton, T. E. Mallouk and A. Sen, *Angew. Chem., Int. Ed.*, 2005, **44**, 744–746.
3 P. Dhar, Y. Cao, T. R. Kline, P. Pal, C. Swayne, T. M. Fischer, B. Miller, T. E. Mallouk, A. Sen and T. H. Johansen, *J. Phys. Chem. C*, 2007, **111**, 3607–3613.
4 R. Laocharoensuk, J. Burdick and J. Wang, *ACS Nano*, 2008, **2**, 1069–1075.
5 S. Sundararajan, P. E. Lammert, A. W. Zudans, V. H. Crespi and A. Sen, *Nano Lett.*, 2008, **8**, 1271–1276.
6 A. Maye, C. Hsieh, G. Sugihara and B. Brembs, *PLoS One*, 2007, **2**, e443.
7 T. W. Engelmann, *Pfluegers Arch.*, 1881, **25**, 285–292.
8 T. W. Engelmann, *Pfluegers Arch.*, 1883, **42**, 183–186.
9 W. Pfeffer, *Untersuch. Bot. Inst. Tubingen*, 1888, **2**, 582.
10 J. P. Armitage and K. J. Hellingwerf, *Photosynth. Res.*, 2003, **76**, 145–155.
11 N. Andrew and R. H. Insall, *Nat. Cell Biol.*, 2007, **9**, 193–200.
12 M. Dekker, in *Interfacial Electrokinetics and Electrophoresis*, ed. Angel V. Delgado, CRC, New York, 2002, vol. 106.
13 S. N. Rasuli and R. Golestanian, *Phys. Rev. Lett.*, 2008, **101**, 108301.
14 J. L. Anderson, *Annu. Rev. Fluid Mech.*, 1989, **21**, 61–99.
15 R. Piazza, *J. Phys.: Condens. Matter*, 2004, **16**, S4195–S4211.
16 B. V. Derjaguin, N. V. Churev and V. M. Muller, *Surface Forces (Engl. Transl.)*, Consultants Bureau, New York, 1987.
17 A. Sen, M. E. Ibele, Y. Hong and D. Velegol, *Faraday Discuss.*, 2009, **143**, 15–27.
18 M. Ibele, T. E. Mallouk and A. Sen, *Angew. Chem., Int. Ed.*, 2009, **48**, 3308–3312.
19 E. M. Purcell, *Am. J. Phys.*, 1977, **45**, 3–11.
20 J. Happell and H. Brenner, *Low Reynolds Number Hydrodynamics*, Prentice Hall, Englewood Cliffs, 1965.
21 A. Najafi and R. Golestanian, *Phys. Rev. E: Stat., Nonlinear, Soft Matter Phys.*, 2004, **69**, 062901.
22 R. Golestanian, T. B. Liverpool and A. Ajdari, *New J. Phys.*, 2007, **9**, 126.
23 D. Fleishman, J. Klafter, M. Porto and M. Urbakh, *Nano Lett.*, 2007, **7**, 837–842.
24 J. E. Avron, O. Kenneth and D. H. Oaknin, *New J. Phys.*, 2005, **7**, 234–242.
25 C. M. Pooley, G. P. Alexander and J. M. Yeomans, *Phys. Rev. Lett.*, 2007, **99**, 228103.
26 R. Golestanian, *Phys. Rev. Lett.*, 2008, **100**, 038101.
27 U. M. Córdova-Figueroa and J. F. Brady, *Phys. Rev. Lett.*, 2008, **100**, 158303.
28 W. F. Paxton, S. Sundararajan, T. E. Mallouk and A. Sen, *Angew. Chem., Int. Ed.*, 2006, **45**, 5420–5429.
29 R. Dreyfus, J. Baudry, M. L. Roper, M. Fermigier, H. A. Stone and J. Bibette, *Nature*, 2005, **437**, 862–865.
30 S. Nakata and K. Matsuo, *Langmuir*, 2005, **21**, 982–984.
31 Y. Osada, J. P. Gong, M. Uchida and N. Isogai, *Jpn. J. Appl. Phys.*, 1995, **34**, L511–L512.
32 J. P. Gong, S. Matsumoto, M. Uchida, N. Isogai and Y. Osada, *J. Phys. Chem.*, 1996, **100**, 11092–11097.
33 T. Mitsumata, J. P. Gong and Y. Osada, *Polym. Adv. Technol.*, 2001, **12**, 136–150.
34 N. Bassik, B. T. Abebe and D. H. Gracias, *Langmuir*, 2008, **24**, 12158–12163.
35 D. Okawa, S. J. Pastine, A. Zettl and J. M. J. Fréchet, *J. Am. Chem. Soc.*, 2009, **131**, 5396–5398.
36 C. D. Bain, *ChemPhysChem*, 2001, **2**, 580–582.
37 R. J. Dijkink, J. P. van der Dennen, C. D. Ohl and A. Prosperetti, *J. Micromech. Microeng.*, 2006, **16**, 1653–1659.
38 J. Vicario, R. Eelkema, W. R. Browne, A. Meetsma, R. M. La Crois and B. L. Feringa, *Chem. Commun.*, 2005, 3936–3938.
39 D. Pantarotto, W. R. Browne and B. L. Feringa, *Chem. Commun.*, 2008, 1533–1535.
40 L. A. Cameron, M. J. Footer, A. van Oudenaarden and J. A. Theriot, *Proc. Natl. Acad. Sci. U. S. A.*, 1999, **96**, 4908–4913.
41 R. F. Ismagilov, A. Schwartz, N. Bowden and G. M. Whitesides, *Angew. Chem., Int. Ed.*, 2002, **41**, 652–654.
42 W. F. Paxton, K. C. Kistler, C. C. Olmeda, A. S. S. K. S. Angelo, Y. Cao, T. E. Mallouk, P. E. Lammert and V. H. Crespi, *J. Am. Chem. Soc.*, 2004, **126**, 13424–13431.
43 W. F. Paxton, A. Sen and T. E. Mallouk, *Chem.–Eur. J.*, 2005, **11**, 6462–6470.
44 W. F. Paxton, P. T. Baker, T. R. Kline, Y. Wang, T. E. Mallouk and A. Sen, *J. Am. Chem. Soc.*, 2006, **128**, 14881–14888.
45 T. R. Kline, W. F. Paxton, T. E. Mallouk and A. Sen, *Developing Catalytic Nanomotors*, Springer, New York, 2007, vol. 3.
46 U. K. Demirok, R. Laocharoensuk, K. M. Manesh and J. Wang, *Angew. Chem., Int. Ed.*, 2008, **47**, 9349–9351.
47 Y. Wang, R. M. Hernandez, D. J. Bartlett, J. M. Bingham, Jr., T. R. Kline, A. Sen and T. E. Mallouk, *Langmuir*, 2006, **22**, 10451–10456.
48 M. E. Ibele, Y. Wang, T. R. Kline, T. E. Mallouk and A. Sen, *J. Am. Chem. Soc.*, 2007, **129**, 7762–7763.
49 N. Mano and A. Heller, *J. Am. Chem. Soc.*, 2005, **127**, 11574–11575.
50 L. Steinbrecher and W. S. Hall, *Process for Coating Metals*, Amchem Products, Inc., 1971.
51 D. C. Prieve, H. L. Gerhart and R. E. Smith, *Ind. Eng. Chem. Prod. Res. Dev.*, 1978, **17**, 32–36.
52 R. Piazza and A. Parola, *J. Phys.: Condens. Matter*, 2008, **20**, 153102–153119.
53 M. Giglio and A. Vendramini, *Phys. Rev. Lett.*, 1977, **38**, 26–30.
54 J. K. G. Dhont, S. Wiegand, S. Duhr and D. Braun, *Langmuir*, 2007, **23**, 1674–1683.
55 S. Duhr and D. Braun, *Proc. Natl. Acad. Sci. U. S. A.*, 2006, **103**, 19678–19682.

56 R. D. Leonardo, F. Ianni and G. Ruocco, *Langmuir*, 2009, **25**, 4247–4250.
57 C. Chevalier, F. Debbasch and J. P. Rivet, *Mod. Phys. Lett. B*, 2009, **23**, 1147–1155.
58 B. V. Derjaguin, G. P. Sidorenko, E. A. Zubashenko and E. B. Kiseleva, *Colloid J. USSR*, 1947, **9**, 335–348.
59 S. S. Dukhin and B. V. Derjaguin, *Electrokinetic Phenomena*, John Wiley and Sons, New York, 1974.
60 B. R. Martin, S. K. S. Angelo and T. E. Mallouk, *Adv. Funct. Mater.*, 2002, **12**, 759–765.
61 R. Golestanian, T. B. Liverpool and A. Ajdari, *Phys. Rev. Lett.*, 2005, **94**, 220801.
62 C. E. Snyder, A. M. Yake, J. D. Feick and D. Velegol, *Langmuir*, 2005, **21**, 4813–4815.
63 A. M. Yake, R. A. Panella, C. E. Snyder and D. Velegol, *Langmuir*, 2006, **22**, 9135–9141.
64 J. J. McDermott and D. Velegol, *Langmuir*, 2008, **24**, 4335–4339.
65 R. Golestanian, *Phys. Rev. Lett.*, 2009, **102**, 188305.
66 H. Watarai, M. Suwa and Y. Iiguni, *Anal. Bioanal. Chem.*, 2004, **378**, 1693–1699.
67 T. M. Vickrey and J. A. Garcia-Ramirez, *Sep. Sci. Technol.*, 1980, **15**, 1297–1304.
68 P. Devreotes and C. Janetopoulos, *J. Biol. Chem.*, 2003, **278**, 20445–20448.
69 J. S. Condeelis, J. B. Wyckoff, M. Bailly, R. Pestell, D. Lawrence, J. Backer and J. E. Segall, *Semin. Cancer Biol.*, 2001, **11**, 119–128.
70 V. Gangur, N. P. Birmingham and T. S, *Vet. Immunolo. Immunopathol.*, 2002, **86**, 127–136.
71 M. A. Moore, *BioEssays*, 2001, **23**, 674–676.
72 P. M. Murphy, *N. Engl. J. Med.*, 2001, **345**, 833–835.
73 S. G. Worthley, J. I. Osende, G. Helft, J. J. Badimon and V. Fuster, *Mt. Sinai J. Med.*, 2001, **68**, 167–181.
74 F. W. Orr, *Adv. Mol. Cell Biol.*, 1994, **9**, 153–189.
75 K. Koizumi, S. Hojo, T. Akashi, K. Yasumoto and I. Saiki, *Cancer Sci.*, 2007, **98**, 1652–1658.
76 H. C. Berg, *Phys. Today*, 2000, **53**, 24–29.
77 D. B. Dusenbery, *Biophys. J.*, 1998, **74**, 2272–2277.
78 J. Adler and W.-W. Tso, *Science*, 1974, **184**, 1292–1294.
79 R. M. Macnab and D. E. Koshland, Jr., *Proc. Natl. Acad. Sci. U. S. A.*, 1972, **69**, 2509–2512.
80 Y. Hong, N. M. K. Blackman, N. D. Kopp, A. Sen and D. Velegol, *Phys. Rev. Lett.*, 2007, **99**, 178103.
81 W. B. Russell, D. A. Saville and W. R. Schowalter, *Colloidal Dispersions*, Cambridge University Press, 1989.
82 D. Ermak and J. A. McCammon, *J. Chem. Phys.*, 1978, **69**, 1352.
83 C. Arrieumerlou and T. Meyer, *Dev. Cell*, 2005, **8**, 215–227.
84 R. T. Tranquillo, D. A. Lauffenburger and S. H. Zigmond, *J. Cell Biol.*, 1988, **106**, 303–309.
85 M. Bornens, *New Biol.*, 1991, **3**, 627–636.
86 J. E. Segall, *Curr. Biol.*, 1999, **9**, R46–R48.
87 L. Stephens, L. Milne and P. Hawkins, *Curr. Biol.*, 2008, **18**, R485–R494.
88 R. L. Stavis and R. Hirschberg, *J. Cell Biol.*, 1973, **59**, 367–377.
89 G. D. Geske, J. C. O'Neill and H. E. Blackwell, *Chem. Soc. Rev.*, 2008, **37**, 1432–1447.
90 S. R. Chhabra, B. Philipp, L. Eberl, M. Givskov, P. Williams and M. Cámara, *Top. Curr. Chem.*, 2005, **240**, 279–315.
91 K. J. Hellingwerf, *Trends Microbiol.*, 2005, **13**, 152–158.
92 Y. Gu and D. Li, *J. Colloid Interface Sci.*, 2000, **226**, 328–339.
93 S. F. Gilbert, *Developmental Biology*, Sinauer Associates, Sunderland, MA, 2006, 8th edn, pp. 36–39.
94 Y. Hong, M. Diaz, U. Córdova-Figueroa and A. Sen, *Nano Lett.*, 2009.
95 O. B. Usta, A. Alexeev, G. Zhu and A. C. Balazs, *ACS Nano*, 2008, **2**, 471–476.
96 A. Kentsis, *Nature*, 2006, **441**, E5.